Food and Chemical Toxicology 124 (2019) 30–44

Contents lists available at ScienceDirect

Food and Chemical Toxicology

journal homepage: www.elsevier.com/locate/foodchemtox

Ganoderma tsugae induced ROS-independent apoptosis and cytoprotective autophagy in human chronic myeloid leukemia cells

You-Cheng Hseu[a,b,c,d], Yi-Chun Shen[e], Ming-Ching Kao[f], Dony Chacko Mathew[a], Palaniyandi Karuppaiya[e], Mei-Ling Li[e], Hsin-Ling Yang[e,*]

[a] Department of Cosmeceutics, College of Biopharmaceutical and Food Sciences, China Medical University, Taichung, 40402, Taiwan
[b] Department of Health and Nutrition Biotechnology, Asia University, Taichung, 41354, Taiwan
[c] Chinese Medicine Research Center, China Medical University, Taichung, 40402, Taiwan
[d] Research Center of Chinese Herbal Medicine, China Medical University, Taichung, 40402, Taiwan
[e] Institute of Nutrition, College of Biopharmaceutical and Food Sciences, China Medical University, Taichung, 40402, Taiwan
[f] Department of Biological Science and Technology, College of Biopharmaceutical and Food Sciences, China Medical University, Taichung, 40402, Taiwan

ARTICLE INFO

Keywords:
Ganoderma tsugae
Human chronic myeloid leukemia
G2/M arrest
Apoptosis
Autophagy

ABSTRACT

The medicinal fungus *Ganoderma*, known in Chinese as Lingzhi or Reishi, traditionally has various medicinal uses and has been employed in cancer treatment in Asia for centuries. This study used ethanol-extracted *Ganoderma tsugae* (GT) and examined its antitumor activities on human chronic myeloid leukemia cells as well as its molecular mechanism of action. Treatment with GT (200–400 μg/mL) significantly reduced cell viability and caused G2/M arrest in K562 cells. In addition, GT induced mitochondrial and death receptor mediated apoptosis, correlated with DNA fragmentation, followed by cytochrome c release, caspase-3/8/9 activation, PARP cleavage, Fas activation, Bid cleavage, and Bax/Bcl-2 dysregulation. Cytoprotective autophagy was found to be induced by GT, as was revealed by increased LC3-II accumulation, Beclin-1/Bcl-2 dysregulation, acidic vesicular organelle formation, and p62/SQSTM1 activation. Notably, pretreatment of cells with the autophagy inhibitors 3-MA and CQ enhanced GT-induced apoptosis. Interestingly, reactive oxygen species production in cells was not triggered by GT administration; equally, the antioxidant *N*-acetylcysteine was found to be incapable of preventing apoptosis and autophagy induced by GT treatment. Finally, this study discovered that cytoprotective autophagy induced by GT was associated with EGFR and PI3K/AKT/mTOR signaling cascade suppression. In summary, GT demonstrated antitumor activity against human chronic myeloid leukemia.

1. Introduction

Chronic myeloid leukemia (CML) is one of the deadliest malignant hematological stem-cell disorders in adults and is characterized by myeloid proliferation and Philadelphia chromosomal aberration (Nowell, 2007). For most patients with CML, allogeneic hematopoietic stem-cell transplantation and tyrosine kinase inhibitor (TKI) therapy are the accepted treatment. However, a few such patients fail to respond to TKIs because of their genetic mutations. Patients who undergo TKI therapy often report cutaneous side effects (Webb et al., 2017). Phytocomponents are receiving increasing attention in the field of cancer biology due to their minor or nontoxicity and cost effectiveness. Scholars are thus currently investigating whether natural products could be invaluable for the treatment of cancer and infection. Accumulating evidence has been obtained that a variety of phytochemicals such as alkaloids, saponins, flavonoids, terpenoids, lignans, saponins, peptides, polyketides, and plant extracts inhibit CML proliferation and induce apoptosis (Khajapeer and Baskaran, 2016). Therefore, the development of novel drugs or agents from natural resources is critical to generating therapeutic regimens for patients with CML.

Clinical trials have evaluated the anticarcinogenic property of medicinal mushroom extracts (Lu et al., 2016). Polysaccharides derived from medicinal mushrooms are best known for their anticancer and immunomodulatory properties. In addition, scholars have demonstrated that these phytocompounds and extracts from medicinal mushrooms induce apoptosis, autophagy, and cell-cycle arrest in various types of cancerous cells and can be used as a chemotherapeutic

* Corresponding author. Institute of Nutrition, College of Biopharmaceutical and Food Sciences, China Medical University, 91 Hsueh Shih Road, Taichung, 40402, Taiwan.
E-mail address: hlyang@mail.cmu.edu.tw (H.-L. Yang).

https://doi.org/10.1016/j.fct.2018.11.043
Received 27 July 2018; Received in revised form 18 October 2018; Accepted 18 November 2018
Available online 19 November 2018
0278-6915/

agent (Hsu et al., 2008; Patel and Goyal, 2012; Wang et al., 2017; Wu et al., 2012; Yu et al., 2012). Eukaryotic cell-cycle progression is a fundamental mechanism determining cell proliferation; the subsequent activation of cyclin-dependent kinases and cyclin is known to mediate this mechanism (Pan et al., 2002). Several chemotherapeutic agents have been derived from non-toxic natural products, and these agents inhibit cell growth and proliferation in cancerous cells through prompting cell-death signaling cascades (Ricci and Zong, 2006).

Apoptosis and autophagy play crucial physiological and pathological roles in numerous diseases including cancer and are part of a sequence of biochemical events that cause changes to cell structure and eventually resulting in cell death. During apoptosis, chromatin is condensed, caspases are activated, and internucleosomal DNA is cleaved (Taylor et al., 2008). Autophagy involves the degradation of long-standing cytosolic proteins and organelles as well as material recycling for maintaining cellular component quality (Maiuri et al., 2007). However, exaggerated autophagy leads to programmed cell death of type II; this is because mitochondria and other survival molecules are intensely degraded (Morselli et al., 2009). Drugs and treatments against cancer cause cellular death in cancer cells by triggering autophagy rather than apoptosis (Gozuacik and Kimchi, 2004; Kondo et al., 2005). How apoptosis and autophagy proceed simultaneously is complex and dependent on the cellular context. Accumulating evidence indicates that excessive reactive oxygen species (ROS) relentlessly damage DNA and proteins and reduce the potential of the mitochondrial membrane potential ($\Delta\Psi m$), leading to apoptosis and autophagy (Ly et al., 2003; Park et al., 2012). Thus, the main objectives of chemoprevention are blocking cancer-cell initiation and promotion and inducing either or both autophagy and apoptosis (Sharma, 2012).

Used in traditional Chinese medicine for more than 4000 years in Asian countries, *Ganoderma*, a popular chemopreventive medicinal mushroom genus, has recently strongly garnered the attention of Taiwan's cancer research (and more broadly, health care) communities (Hsu et al., 2008; Yu et al., 2012). Of the numerous bioactive compounds that are present in mushrooms of this genus, polysaccharides and triterpenoids are the most promising for therapy against many diseases, cancer being one (Zhou et al., 2007). *Ganoderma tsugae* (GT), a medicinal fungus, has had a role within Taiwanese folk medicine for a long time (Hsu et al., 2008; Yu et al., 2012) and has demonstrated strong anti-inflammatory (Ko et al., 2008), antioxidant (Tseng et al., 2008), antifibrotic (Zhou et al., 2007), and anticancer (Yu et al., 2012) effects. The growth-inhibitory effects of GT on colorectal cancer cells (Hsu et al., 2008), epidermoid carcinoma cells (Hsu et al., 2009), breast cancer cells (Yue et al., 2006), hepatoma cells (Gan et al., 1998), HER2-overexpressing cancer cells (Kuo et al., 2013), and lung adenocarcinoma cells (Yu et al., 2012), among other cell types, have previously been demonstrated. In our previous studies, which employed high-performance liquid chromatography (HPLC) and thin-layer chromatography, we determined the chemical components of GT and how the triterpenoids it contains are different from those of other *Ganoderma* species (Su et al., 2001; Hsu et al., 2009).

The present study investigated the effect of GT on autophagy and/or apoptosis in human CML (K562) cells, because this effect is considered to have excellent effectiveness in treatment of cancer. Compelling evidence has been obtained that GT extracts induce anticancer activity in various cancer cells through cell-death signaling cascades. However, no studies have yet investigated the effects of these extracts on autophagy and apoptosis in the particular cell type examined in the present work.

2. Materials and methods

2.1. Reagents and antibodies

Penicillin, streptomycin, Roswell Park Memorial Institute medium (RPMI-1640), Iscove's modified Dulbecco's medium (IMDM), glutamine, and fetal bovine serum (FBS) were sourced from Gibco-BRL (NY, USA). From Santa Cruz Biotechnology, Inc. (Heidelberg, Germany), we obtained mouse monoclonal antibodies against Bax and β-actin and rabbit polyclonal antibodies against cytochrome c, Bcl-2, Fas, and β-tubulin. Mouse monoclonal antibodies against Bid were procured from Cell Signaling Technology, Inc. (MA, USA), as were rabbit monoclonal antibodies against caspase-3, caspase-8, caspase-9, Bax, and PARP. Antibodies against Beclin-1, p62/SQSTM1, p-mTOR, p-PI3K, PI3K, LC3I/II, AKT, and p-AKT came from Cell Signaling Technology, Inc. Antibody against p-EGFR was from Life Technologies (Gaithersburg, MD, USA). Antibody against GAPDH was procured from Cusabio Biotechnology, Inc. (Wuhan, China). All secondary antibodies were bought from Santa Cruz Biotechnology (CA, USA). The chemicals 3-methyladenine (3-MA), 3-(4,5-dimethylthiazol-2-yl)-2,5-diphenyltetrazolium bromide (MTT), *N*-acetylcysteine (NAC), propidium iodide (PI), acridine orange (AO), chloroquine (CQ), and 2‘, 7‘-dihydrofluorescein-diacetate ($DCFH_2$-DA) were from Sigma-Aldrich (MO, USA). We obtained Z-Val-Ala-Asp-fluoromethylketone (z-VAD-FMK) from Calbiochem (CA, USA). The remaining chemicals used in this experiment were reagent or HPLC grade and were obtained from Sigma-Aldrich or Merck & Co., Inc. (Darmstadt, Germany).

2.2. Ganoderma tsugae extract preparation

Ganoderma tsugae was generously gifted by Luo-Gui Ying of the Fungi Agriculture Farm in Taoyuan, Taiwan. GT extracts were derived using a method reported earlier (Hsu et al., 2008). The extracts were standardized as mentioned by Tseng et al. (2018) (Tseng et al., 2018). In brief, a powder of the fruiting body of GT (30 g) was immersed in 300 mL of 99.9% ethanol, with the solution then mixed and shaken using a rotating shaker for 24 h. After being centrifuged, the filtrate underwent filtering using filter paper (Whatman, cat. No. 1001–110) and the residues were extracted with ethanol two times. The collected filtrates were concentrated in a rotary evaporator under reduced pressure. The yield of the GT extracts was approximately 13.8%. GT stock solution was prepared with ethanol (200 mg/mL) and, until further use, stored at −80 °C.

2.3. Cell culture

Human leukemic cell lines were obtained (U937, HL-60, and K562) from the American Type Culture Collection (ATCC; MD, USA). K562 cells were cultured in IMDM, whereas we cultured cells of type HL-60 and U937 were cultured in RPMI-1640. Both the IMDM and RPMI-1640 medium contained 2 mM glutamine, 10% heat-inactivated FBS, and 1% penicillin–streptomycin–neomycin. All culturing occurred at 37 °C in a 5% CO_2 humidified incubator. A hemocytometer was employed to count the number of harvested cells. Trypan blue exclusion was employed to calculate the cell viability (1×10^5 cells/mL) before treatment with GT as well as after.

2.4. MTT assay

Briefly, human leukemia cell lines were exposed (1×10^5 cells/well in 24-well plates) to various concentrations of GT (200, 300, or 400 μg/mL) for 24 h. To each well was added 1 mL of 0.5 mg/mL MTT in phosphate-buffered saline (PBS), after which the cells were incubated for 1 h at 37 °C. After incubation, an equal volume of DMSO (0.8 mL) was added, which dissolved the MTT formazan crystals. An enzyme-linked immunosorbent assay microplate reader (μ-Quant, VT, USA) was employed to measure the absorbance (570 nm). All measurements were performed in triplicate. Cell viability (%) was calculated as (A_{570} of treated cells/A_{570} of untreated cells) × 100.

2.5. Flow cytometric analysis

A single-ion laser–equipped (488 nm) FACScalibur flow cytometer

(Becton Dickinson, CA, USA) was employed for flow cytometry. The PI-labeled cells were subjected to flow cytometric analyses to determine cellular DNA levels, as detailed in a previous study (Hseu et al., 2008). Briefly, 1×10^5 cells/mL was cultured in culture dishes measuring 10 cm. After GT treatment, we harvested and then washed the cells. Subsequently, they were suspended in PBS and underwent fixation in ice-cold 70% ethanol; they were then kept overnight at −20 °C. The next day, these cells were resuspended in PBS containing 4 μg/mL PI, 1% Triton X-100, and 0.5 mg/mL RNase at 37 °C for 30 min after incubation. To analyze the cell cycle, ModFit software was used. Sub-diploid DNA peaks identified apoptotic nuclei, and forward light scattering and PI fluorescence were used to distinguish these nuclei from cell debris.

2.6. TUNEL assay

To calculate the degree of apoptotic cell death, we employed an *in situ* cell-death detection kit (Millipore, MA, USA), as per manufacturer instructions, for terminal deoxynucleotidyl transferase-mediated dUTP-fluorescein nick end-labeling (TUNEL), as detailed elsewhere (Yang et al., 2013). In brief, following treatment with GT (200, 300, or 400 μg/mL), we harvested apoptotic K562 cells (1×10^5 cells/mL) and fixed them with 4% formaldehyde for 1 h followed by 1 μg/mL DAPI for 15 min at 37 °C. To detect apoptosis, we labeled the 3'OH ends of the fragmented DNA with biotin-dNTP by using the Klenow fragment at 37 °C for 1.5 h. Nuclei fluorescence, as detected using a fluorescence microscope, was employed to identify fragmented DNA. A square section of the stained cells were analyzed using LS 5.0 soft image solution (Olympus, PA, USA), and this analysis yielded the fluorescence intensity. The percentage of apoptotic cell death, which is proportional to fluorescence intensity, was determined by comparing the fluorescence intensities of the treated cells and untreated control cells.

2.7. Measurement of ROS generated

Fluorescence microscopy with a cell-permeable fluorogenic probe $DCFH_2$-DA was employed to detect the accumulation of ROS in cells. The cells (1×10^5 cells/mL) were cultured in IMDM supplemented with 10% FBS; once 80% confluency had been achieved, the medium was replaced. To evaluate the ROS that were generated at different time points, the cells were treated with 300 μg/mL GT for 15–120 min. This was followed by the removal of the cell culture supernatant and the addition of fresh medium containing 10 μM $DCFH_2$-DA; the cells were then incubated at 37 °C for 30 min. The oxidation of $DCFH_2$ caused accumulation of dichlorofluorescein (DCF) in cells, which in turn resulted in the changes in fluorescence used to quantify ROS production. A fluorescence microscope (200 ×) (Olympus, PA, USA) was employed to image the cells fluorescently stained with DCF. A square section of fluorescently stained cells were analyzed using analySIS LS 5.0 soft image solution (Olympus, PA, USA) to quantify the fluorescence intensity. We compared the fluorescence intensities of the treated cells and untreated control cells to determine the ROS generated.

2.8. Analysis of mitochondrial membrane potential

Flow cytometry was employed to assess the mitochondrial membrane potential. The cells were (1×10^5 cells/mL in dishes of size 10 cm) and washed twice, after which resuspended them in $DiOC_6$ (500 mL; 20 mM) and incubated for 30 min at 37 °C, the excitations were monitored at 530 nm ($DiOC_6$). ModFit software was used to calculate cell percentages.

2.9. Annexin V/PI staining assay

K562 cells were treated with GT (200–400 μg/mL) for a period between 0 and 24 h. Subsequently, the cells were harvested, washed twice with PBS, and centrifuged for 5 min at 800 rpm. Binding buffer (100 μL) was employed to suspend the cells (1×10^5 cells/mL). Them, the cells were stained with both Annexin V-FITC and a PI Apoptosis Detection kit (Biovision, CA, USA) per manufacturer protocol. The reaction of Annexin V-FITC and PI binding was quantitatively analyzed using a FACScalibur flow cytometer (Becton Dickinson) and CellQuest software.

2.10. Acidic vesicular organelle observation using AO assay

K562 cells were stained with AO to observe acidic vesicular organelles (AVOs) formed in the cells. After GT treatment, the cells underwent two PBS washings, AO staining (1 μg/mL), and 15-min dilution in PBS containing 5% FBS. Subsequently, we washed the cells with PBS and covered them with a solution of PBS and 5% FBS. A fluorescence microscope at 200 × magnification was used to visualize AVOs in cells, and flow cytometry was employed for subsequent analysis. A lysosomotropic metachromatic fluorescent dye, AO has concentration-dependent fluorescence emission; at high concentrations (in lysosomes), it emits red light; at intermediate concentrations, yellow (under some conditions only); at low concentrations (in the cytosol), green.

2.11. Western blotting analysis

K562 cells (1×10^5 cells/mL) were incubated with or without GT (200–400 μg/mL) for certain time periods. Postincubation, we harvested the cells and washed them once with PBS. Subsequently, they were suspended in lysis buffer (100 μL; 10 mM Tris-HCL, pH 8; 320 mM sucrose, 1% Triton X-100, 5 mM EDTA, 2 mM DTT and 1 mM PMSF). We maintained the cell lysates on ice for 20 min and subjected them to 15,000-*g* centrifugation at 4 °C for 30 min. Bio-Rad protein assay reagent (Bio-Rad, CA, USA) was employed to determine the total protein level, with bovine serum albumin serving as a standard. A protein extract was mixed with sample buffer (62 mM Tris-HCL, 10% glycerol, 5% β-mercaptoethanol, and 2% sodium dodecyl sulfate (SDS)) and boiled at 97 °C for 5 min. We used 15% SDS–PAGE to separate denatured protein samples (50 μg), and after separation, they were transferred to polyvinylidene difluoride membranes to rest overnight at 4 °C. Next, we blocked the membranes at room temperature for 1 h by using 5% non-fat dried milk in PBS that contained 1% Tween-20, after which the samples underwent overnight incubation with primary antibody at 4 °C. Finally, the primary-antibody-stained membranes were incubated for 2 h with horseradish-peroxidase-conjugated anti-rabbit or anti-mouse antibodies and then stained with chemiluminescent substrate (Millipore). AlphaEase software (FL, USA) was used to perform densitometric analyses, with the control representing a 1-fold increase.

2.12. RNA extraction and RT-PCR

The cells were seeded in a 6-cm dish at the density of 4×10^6 cells/dish. After 90% confluency was reached, the cells were treated for 24 h with GT (200–400 μg/mL). We utilized TRIzol reagent (Invitrogen, NY, USA) to extract RNA from the cultured cells. For reverse transcription–polymerase chain reaction (RT-PCR) (Bio-Rad), 1 μg of total sample RNA was used, with 45 s of amplification for 30–38 cycles at 94 °C, 45 s of annealing at 65 °C, and a 1 min final extension at 72 °C. The primers used were LC3B F: 5′-TTACCTTCCCGAACATCGAC-3′ and LC3B R: 5′-GCATAAATTCCCACTGCCAC-3'. Gel electrophoresis in a 1% agarose gel was used to confirm the PCR products.

2.13. Statistical analysis

Standard deviation is used as the mean to present the results. All experiments were performed in triplicate, and Student's t-test of variance as well as Dunnett's test for pairwise comparisons were used for data analysis. Significant differences in experimental values in

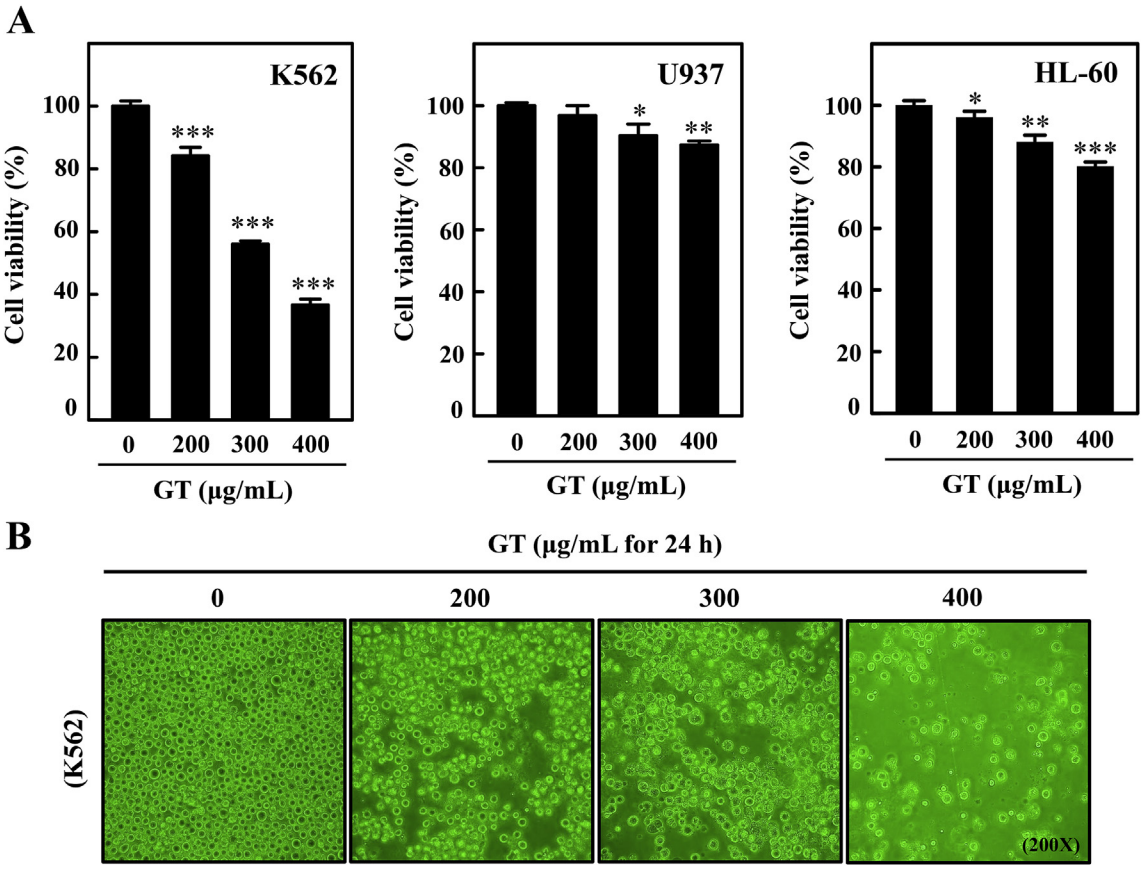

Fig. 1. Inhibition of human CML cell growth by using GT. U937, HL-60, and K562 cells were treated with various GT concentrations (200–400 μg/mL) for 24 h. (A) Cell viability before and after GT treatment was determined through MTT assay. (B) Phase-contrast microscopy (200 × magnification) was used to examine structural changes in GT-treated K562 cells. Data are reported as the mean ± standard deviation (SD) of three experiments. $*p < 0.05$; $**p < 0.01$; $***p < 0.001$ relative to untreated (control) cells.

comparison with control values are denoted by an asterisk ($*p < 0.05$; $**p < 0.01$; $***p < 0.001$).

3. Results

3.1. GT inhibits the growth of human leukemia cells

Previous studies have all portrayed that GT extracts had no cytotoxic effects on normal cell lines and mouse models (Ko et al., 2008; Lin et al., 2006; Chen and Lin, 2007; Kuok et al., 2013). Through MTT, we studied the cytotoxic effects of ethanol extract of GT on human leukemia U937, K562, and HL-60 cell lines. These cells were treated with 200–400 μg/mL of GT for 24 h. GT had significant cytotoxic effects on human chronic myeloid K562 cells (IC_{50} = 320 μg/mL). Particularly, the cytotoxic effect of GT was discovered to be profound in K562 cells in comparison with human monocytic leukemia U937 and promyelocytic leukemia HL-60 cells (Fig. 1A). Therefore, K562 cells were selected for subsequent experiments. In addition, exposure of K562 cells to GT (200–400 μg/mL) resulted in significant shrinking of cells, which was identified using phase-contrast microscopy (Fig. 1B). This study thus obtained evidence that treating K562 cells with GT significantly reduced the rate of proliferation of these cells and induced apoptosis.

3.2. GT caused sub-G_1 accumulation and G_2/M cell-cycle arrest in K562 cells

Through flow cytometry, we measured the fluorescence of PI–DNA complexes, which was then used to assess the DNA levels in GT-treated K562 cells. Compared with the untreated cells, more extensive accumulation of subdiploid cells, a higher sub-G_1 peak, and more extensive apoptosis (blue peak) were observed for the cells treated with GT (200 μg/mL) for 24 h (Fig. 2A and B). By analyzing the cellular distribution during the various phases of post treatment, we identified the cell-cycle stage at which growth was inhibited by GT treatment. GT treatment of K562 cells (Fig. 2B) was discovered to result in progressive and sustained accumulation of cells in the G_2/M phase. The proportion of cells in this phase rose from 16.0% to 23.6% over time; by contrast, that cells in the G_1 and S phases was found to decline (Fig. 2A and B). GT treatment may thus inhibit cell growth through the induction of G_2/M cell-cycle arrest in and apoptosis of K562 cells.

3.3. GT-induced apoptotic DNA fragmentation in K562 cells

Owing to its promising ability to induce death of cancer cells, GT may be assumed to potentially activate the crucial regulatory proteins that participate in apoptosis or autophagy. For further definition of the mechanism through which GT causes cell death, K562 cells underwent GT (200–400 μg/mL) treatment for 24 h, after which TUNEL assay and DAPI staining were performed. At the 3′-OH ends of nuclei, DNA single-strand breaks were labeled using dUTP-fluorescein, and increased fluorescence intensity was discovered, indicating that GT treatment activated apoptosis in K562 cells (Fig. 3A and B). In the control cells, green fluorescence was almost undetectable (1-fold increase), whereas GT-treated cells exhibited significantly higher fluorescence intensity, with the difference in intensity being dose dependent (Fig. 3A and B). A strong DNA fragmentation effect was observed when 300 μg/mL GT treatment was applied, except for 400 μg/mL. Interestingly, 400 μg/mL GT treatment resulted in significantly less DNA fragmentation in

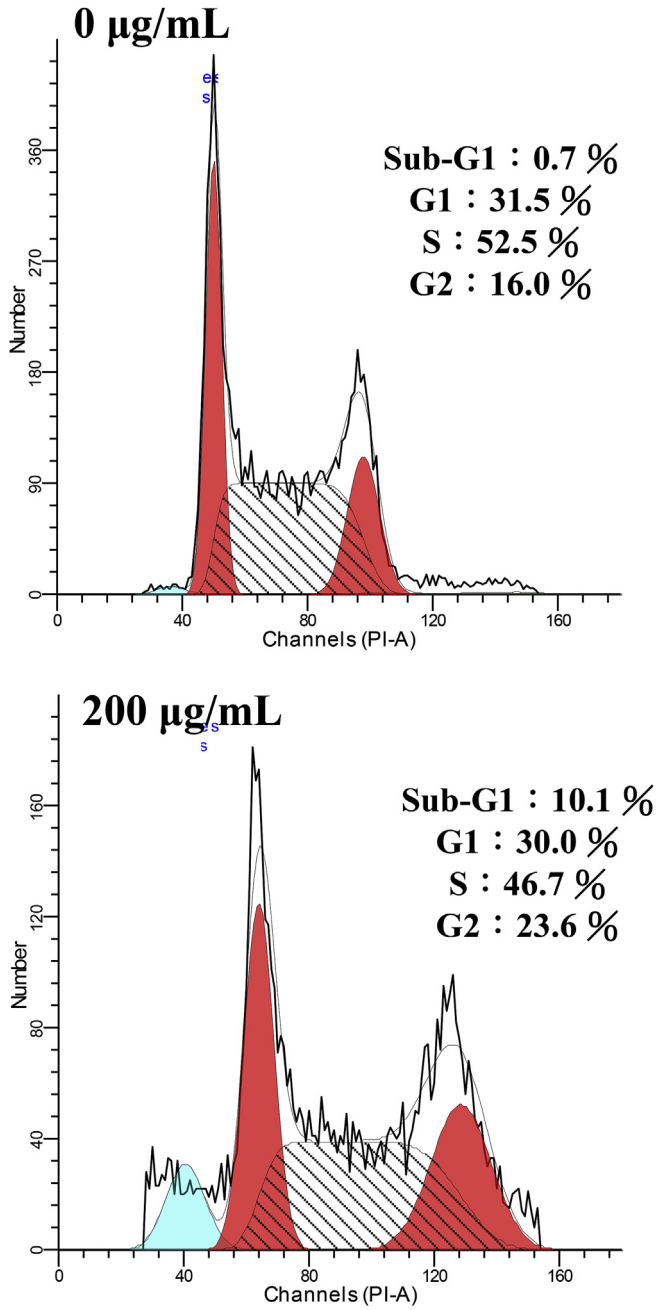

Fig. 2. GT induced G_2 cell-cycle arrest in K562 cells. Fluorescence-activated cell sorting analysis of K562 cells (A) not treated and (B) treated for 24 h with 200 μg/mL of GT. The post-GT-treatment cellular distributions (percentage) for the sub-G1, G1, S, and G2/M cell-cycle phases were obtained. The presented flow cytometry graph is of a representative experiment from among the triplicate.

K562 cells (Fig. 3A and B). These observations demonstrate that GT treatment (200–300 μg/mL) has an effective apoptotic effect on K562 cells.

3.4. GT provokes apoptosis by mitochondrial and death receptor cascades in K562 cells

Because the previous experiment demonstrated that apoptosis could be a factor of cell death, we determined whether the apoptosis was intrinsic or extrinsic. Cytochrome c level in the cytosolic fraction was first found. A 24 h GT treatment (0–300 μg/mL) dose-dependently increased the cytochrome c level in the cytoplasm (Fig. 4A). Subsequently, the effects exerted by GT treatment on the downstream effector cascades of cytochrome c, including caspase-9 and caspase-3, were investigated. Western blotting analysis demonstrated a consequently higher amount of caspase-9 and caspase-3 in GT-treated cells (Fig. 4A). Proteolytic cleavage of PARP by caspase-3 is a key feature of apoptosis; thus, the influence of activated caspase-3 on PARP cleavage was determined. Incubation of cells with GT led to proteolytic cleavage of a PARP fragment from 116 to 89 kDa (Fig. 4A). Overall, these findings (Fig. 4A) suggested that in GT-treated K562 cells, the apoptosis induced by GT occurred concurrently with PARP cleavage, cytochrome c release, and caspase-9/-3 activation.

The next step was to analyze the impact of GT on Fas and caspase-8 proteins. given that these proteins play critical roles in apoptosis mediated by death receptors and extrinsic apoptosis. Using Western blotting, Fas proteins discovered to be significantly and dose-dependently upregulated by GT (0–400 μg/mL for 24 h; Fig. 4B). In addition, GT treatment dose-dependently promoted caspase-8 activation in K562 cells, as indicated by procaspase-8 being cleaved into its active state (Fig. 4B). We also found GT treatment to significantly and dose-dependently down regulate Bid expression (Fig. 4B). Thus, our findings indicated that apoptotic cell death was induced by GT through the mitochondrial pathway (intrinsic apoptosis) and also through the death receptor pathway (extrinsic apoptosis) in human leukemia cells.

3.5. Influence of GT on mitochondrial membrane potential in K562 cells

To determine whether GT treatment reduced the mitochondrial membrane potential, some K562 cells were pretreated for 1 h using ROS inhibitor (NAC, 1 mM), whereas others were not. To both sets of cells, 24-h GT (200–400 mg/mL) treatment was applied, after which the cells underwent $DiOC_6$ staining. Flow cytometry was then employed to determine the mitochondrial membrane potential. GT treatment was discovered to lower the mitochondrial membrane potential (Fig. 4C and D). This finding revealed that mitochondrial dysfunction in K562 cells could be induced by GT.

3.6. Effect of GT on early and late apoptosis in K562 cells

Whether GT promotes necrosis or early/late apoptosis was investigated in this study. Annexin V-FITC and PI assays were performed; in these assays, phosphatidylserine and DNA residues were stained, respectively. As revealed using flow cytometry, 24 h GT treatment (200–400 μg/mL) of K562 cells had a dose-dependent positive effect on the number of early and late apoptotic cells. They were 6.5%, 21.8%, 33.7%, and 86.2% late apoptotic Annexin V/PI double-positive cells represented in Q2 when 0, 200, 300, and 400 μg/mL, respectively, GT treatment was applied (Fig. 5A and B); correspondingly, the percentage of early apoptotic Annexin V/PI double-positive cells represented in Q4 was 4.6%, 21.7%, 19.3%, and 8.1 (Fig. 5A and B). Pretreating cells with 1 mM ROS inhibitor (NAC) did not suppress GT-induced apoptotic events (Fig. 5A and B). However, Z-VAD-FMK pretreatment resulted in significantly reduced GT-induced cell death (Fig. 5C), confirming that in K562 cells, GT induced apoptotic cell death. The presented findings provide novel evidence that GT induces early and late apoptosis in K562 cells, with this effect unaltered by pretreatment with ROS.

3.7. GT activates autophagy by increasing LC3 accumulation in K562 cells

To ascertain whether GT induces autophagy in K562 cells, we studied these cells' distribution of a potentially effective autophagy marker: LC3 I/II (Kabeya et al., 2000). The dose-dependent (0–400 μg/mL) effects of 24 h GT treatment on the LC3-I and LC3-II distributions were identified through Western blotting. The amount of these markers was discovered to be dose-dependently higher after GT treatment. A high GT dose (400 μg/mL) resulted in considerably higher LC3-II accumulation (Fig. 6A). The p62/SQSTM1 expression level was found to

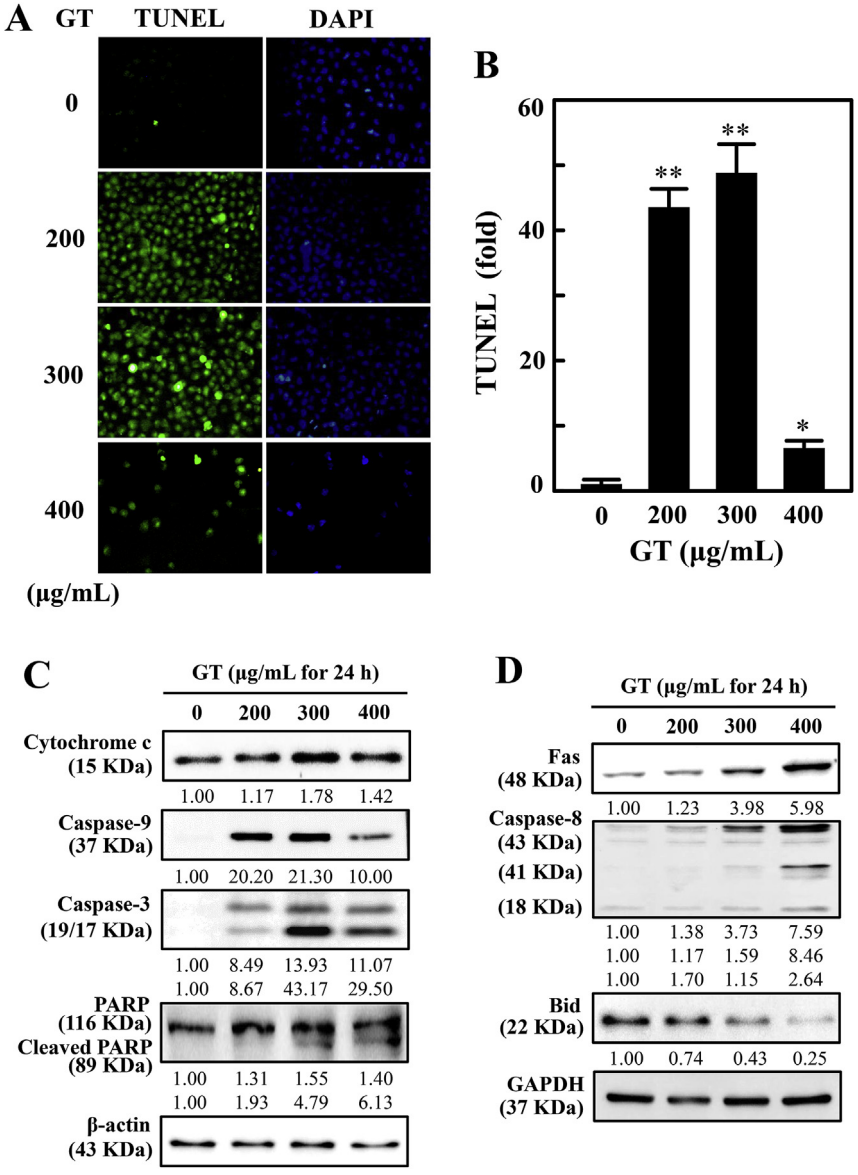

Fig. 3. GT induced cellular apoptosis of K562 cells. (A) Cells that underwent 24-h GT treatment (200–400 μg/mL) were subjected to TUNEL assay. Green fluorescence indicates the number of TUNEL-positive cells in the examined field (400 ×). (B) The fold/percentage increase in apoptotic cells was estimated using the fluorescence intensity of treated cells, which was measured using commercial software. (For interpretation of the references to color in this figure legend, the reader is referred to the Web version of this article.)

be dose-dependently significantly increased after GT incubation (200–400 μg/mL, for 24 h), evidence that autophagy in K562 cells was induced by GT (Fig. 6A). Increased p62/SQSTM1 expression level was correlated with higher accumulation of LC3 (Fig. 6A). RT-PCR showed that GT treatment significantly and dose-dependently increased mRNA expression of LC3, except for when 400 μg/mL of GT was employed (Fig. 6B). The findings strongly suggest that intracellular LC3-I was converted into LC3-II (lipidation) following GT treatment, with the degree of conversion being GT dose dependent; this study thus provides indisputable evidence of autophagy induction in K562 cells by GT.

AVO formation is one of the principal characteristics of autophagy and detected through an increase in the lipidated LC3B level. Because a striking increase in LC3 accumulation was detected in GT-treated K562 cells, GT treatment's further impact on AVO formation was determined by performing AO-staining fluorescence microscopy (Fig. 6C and D). Red fluorescence, corresponding to the presence of AVOs, was GT-dose-dependently stronger in GT-treated K562 cells, except when 400 μg/mL GT was used. This observation revealed a GT-induced autophagic flux in leukemia K562 cells by increasing the amount of LC3 accumulation.

3.8. Activation of autophagy signaling cascade as a survival mechanism in GT-treated K562 cells

The role of GT-induced autophagy in K562 cells was investigated through preventing autophagy by using 3-MA and CQ, which are pharmacological inhibitors that disrupt lysosomal function and prevent autophagy completion. To achieve this goal, cells were treated with GT alone, 3-MA/CQ alone, or both. Cell pretreatment with 3-MA (1 mM) and CQ (20 μM) was found to effectively enhance GT-induced cell death (Fig. 7A and B). These results suggested that autophagy triggered by GT treatment is a mechanism of survival within K562 cells.

3.9. Exclusion of ROS in GT-induced apoptosis and autophagy in K562 cells

We investigated the role of GT in ROS generation within K562 cells.

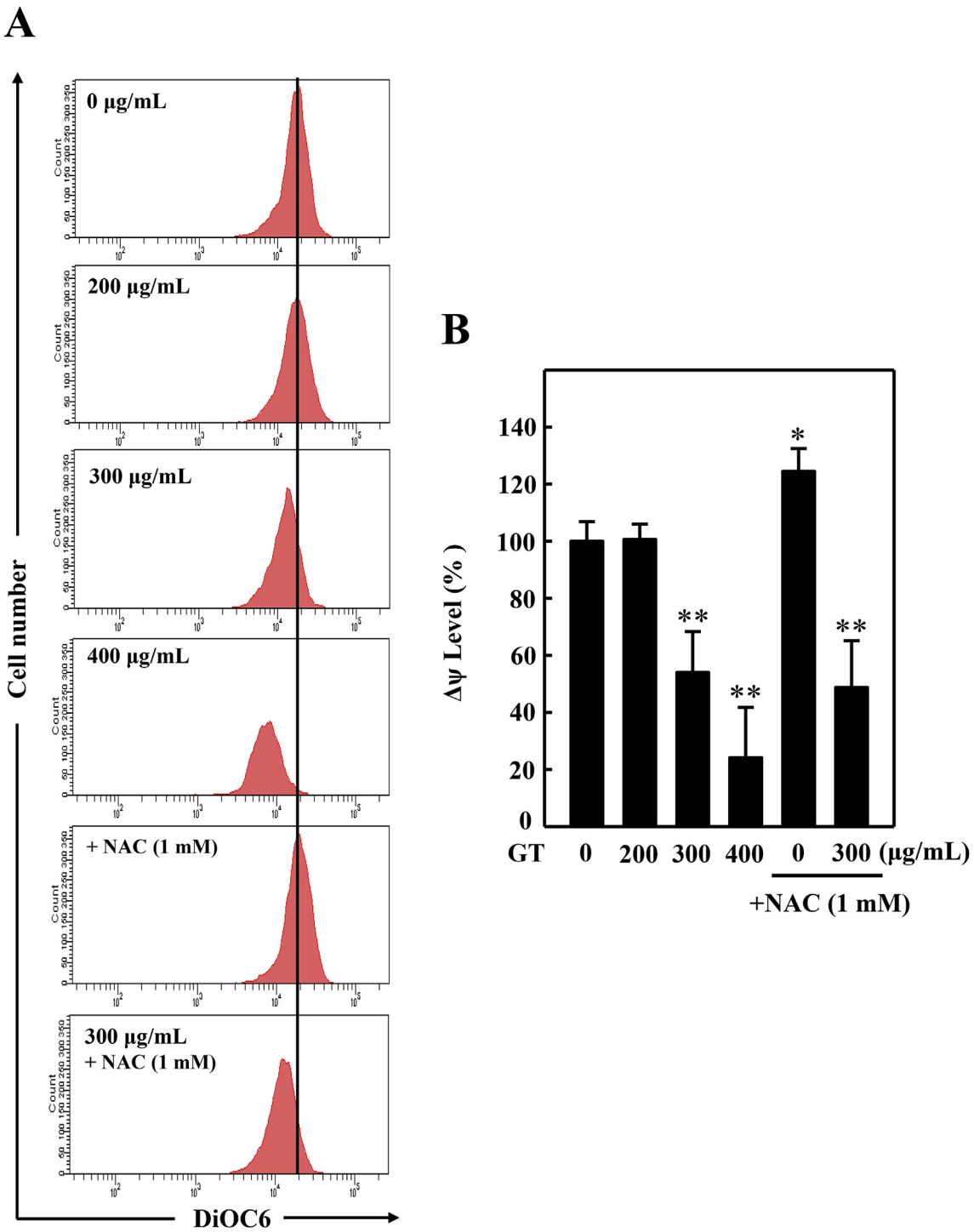

Fig. 4. GT-induced apoptosis in K562 cells was mediated through activating mitochondrial and death receptor pathways, and GT affected the mitochondrial potential. Several concentrations of GT (200–400 μg/mL) were used to treat cells for 24 h (A–B) Protein levels of cytochrome c, caspase-9, caspase-3 and PARP (mitochondrial pathway), Fas, caspase-8, and Bid were assessed in K562 cells by using Western blotting. (C–D) Cells, some undergoing pretreatment with ROS inhibitor (NAC, 1 mM) for 1 h, were treated for 24 h with GT (200–400 mg/mL). (C) Representative flow cytometry patterns obtained after cells were stained with $DiOC_6$ and the staining was evaluated using flow cytometry. (D) The post-GT-treatment mitochondrial membrane potential (% of control), calculated using the degree of $DiOC_6$ fluorescence, is displayed. Data are reported as the mean ± SD of three experiments. $^*p < 0.05$; $^{**}p < 0.01$ relative to untreated cells.

Incubating K562 cells with GT (300 μg/mL) for 15–120 min had no effect on DCF fluorescence (Fig. 8A). To identify whether apoptosis and autophagy induced by GT treatment was ROS-dependent, we incubated K562 cells with 1 mM of an ROS inhibitor (NAC) for 1 h before subjecting them to 400-μg/mL GT treatment. The levels of autophagy markers in the cells were then discovered. Cell viability assay showed that pretreatment of cells with NAC exerted no influence on the degree of GT-induced cell death in K562 cells (Fig. 8B). As shown in Fig. 8C, Western blotting showed cell preincubation with NAC to also have no effects on GT-induced LC3-I/II expression. These findings revealed that ROS may not be involved in GT-induced apoptosis and cytoprotective autophagy in K562 cells.

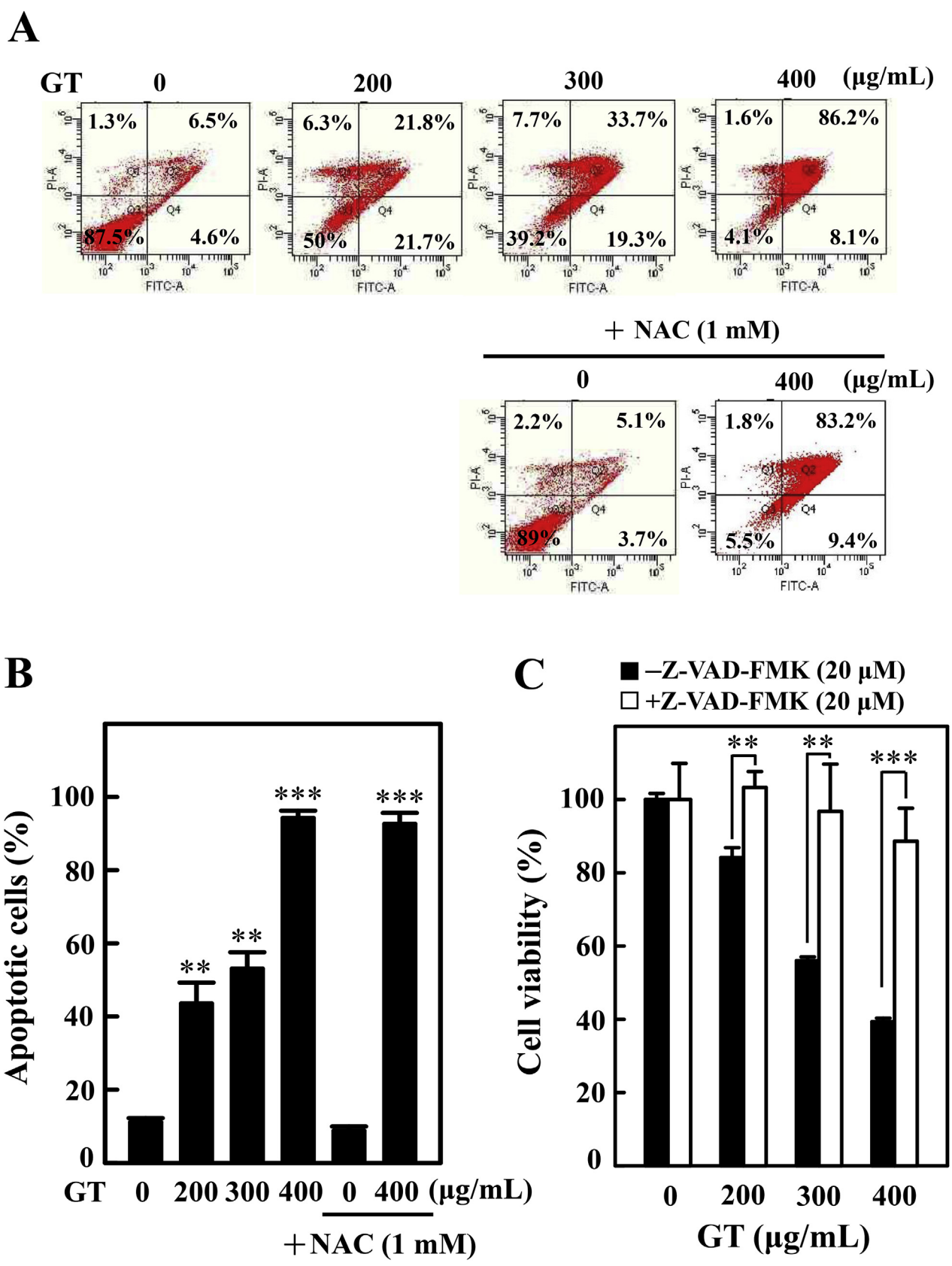

Fig. 5. Cell apoptosis of K562 cells treated with GT. (A) Cells, some undergoing pretreatment with NAC, were treated for 24 h with GT (200–400 μg/mL), stained with Annexin V-FITC and PI-A, and their staining evaluated through flow cytometry. (B) Percentage of cells in which GT-induced apoptosis occurred. (C) K562 cells underwent 1-h pretreatment with pan-caspase inhibitor (Z-VAD-FMK, 20 μM) before being treated with GT (200–400 μg/mL) for 24 h. Cell viability was evaluated through MTT assay. Data are reported as the mean ± SD of three experiments. $^{**}p < 0.01$; $^{***}p < 0.001$ compared with untreated cells.

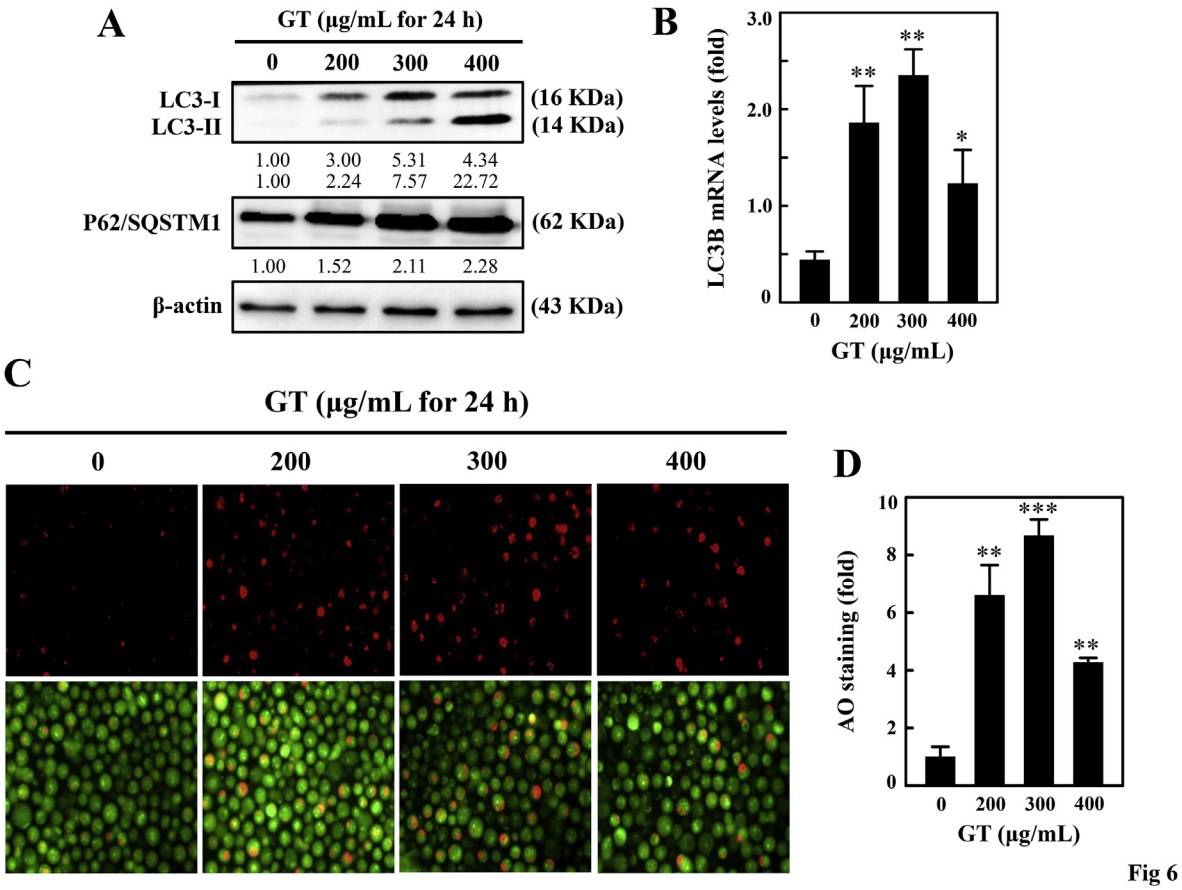

Fig 6

Fig. 6. GT induces autophagy in K562 cells. Cells were treated for 24 h with various GT concentrations (200–400 μg/mL). (A) Protein expression of LC3-I, LC3-II and SQSTM1/p62 assessed using Western blotting. (B) RT-PCR was employed to quantify LC3B mRNA expression levels, which were normalized to that of β-actin. (C) GT induced the formation of AVOs in cells, which was observed using a red filter fluorescence microscope (100 × magnification). Intensity of red fluorescence is proportional to the AVO count in cells. (D) Histogram displaying the number of AO-stained cells following GT treatment subsequent to inhibitor use and nonuse, with the control represented as a 1-fold increase. Data are reported as the mean ± SD of three experiments. $^{**}p < 0.01$; $^{***}p < 0.001$ relative to untreated cells. (For interpretation of the references to color in this figure legend, the reader is referred to the Web version of this article.)

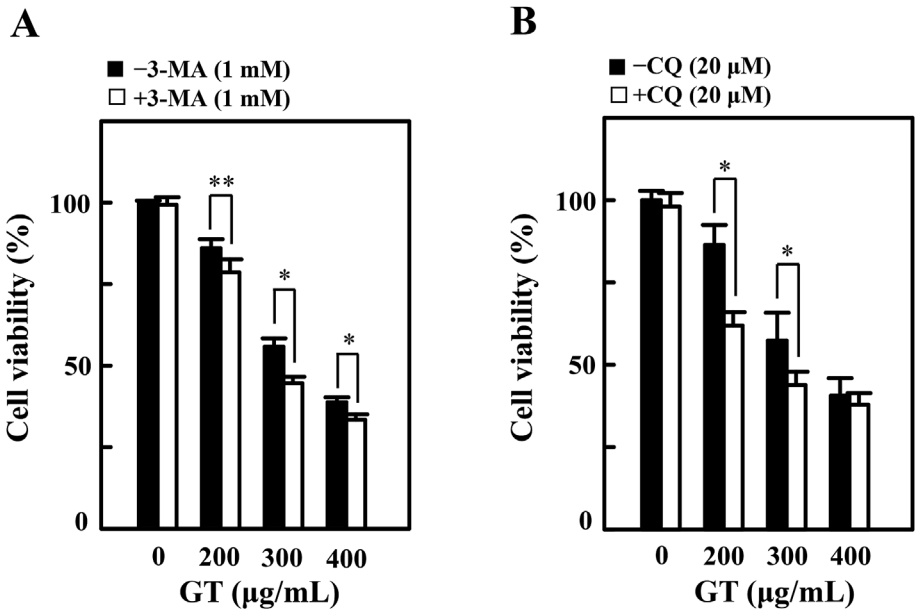

Fig. 7. CQ and 3-MA inhibited GT-induced autophagy in K562 cells. (A–B) Cells were pretreated with 1 mM 3-MA or 20 μM CQ for 1 h, after which they underwent 24-h GT treatment (200–400 μg/mL). Cell viability was evaluated through MTT assay. Data are reported as the mean ± SD of three experiments. $^{**}p < 0.01$; $^{***}p < 0.001$ relative to untreated cells.

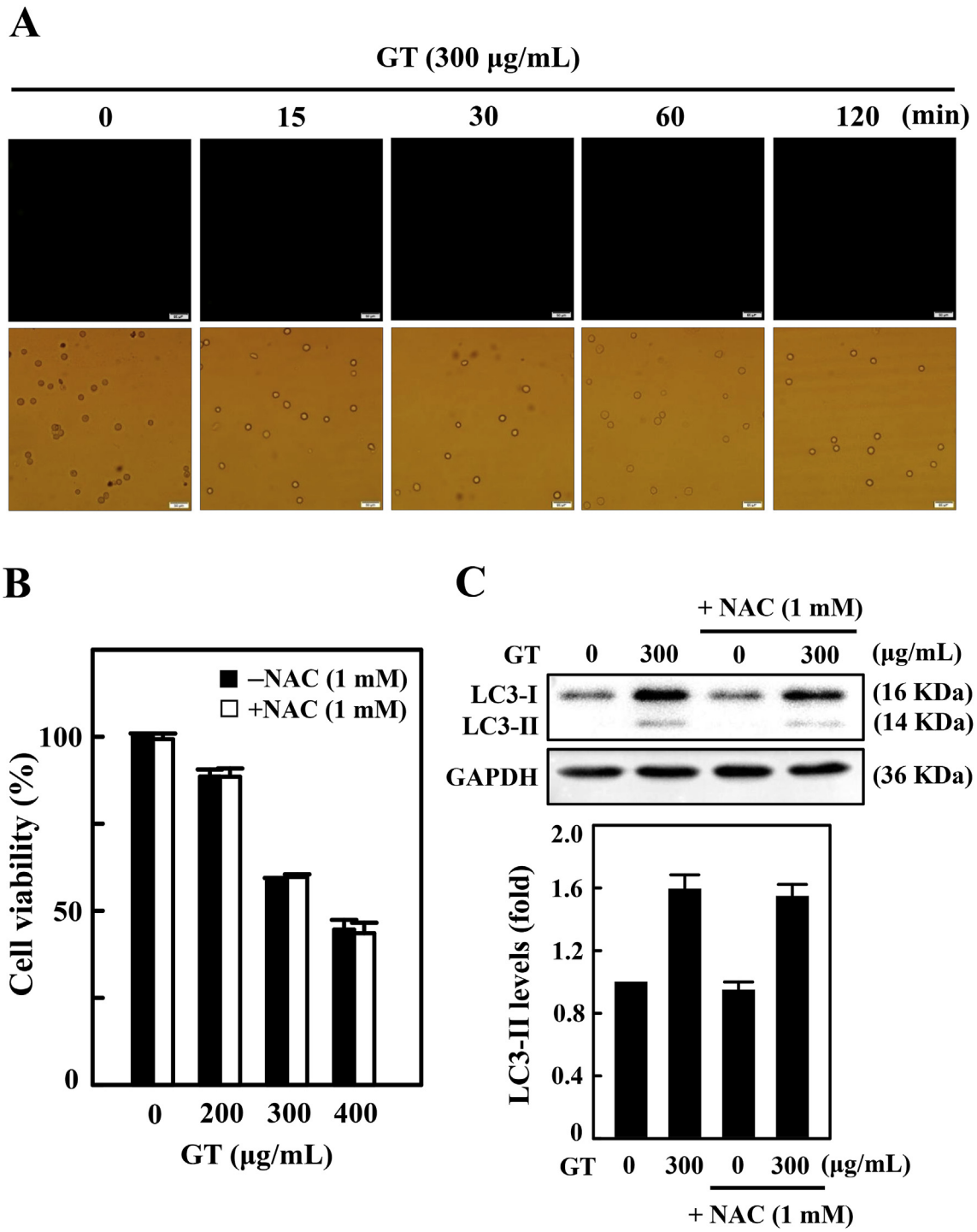

Fig. 8. ROS was not involved in GT-triggered apoptosis and autophagy in K562 cells. (A) Cells underwent 120-min GT treatment (200–400 μg/mL), and the intracellular ROS generated were measured every 15 min during the treatment. $DCFH_2$-DA, a nonfluorescent probe, reacted with cellular ROS, metabolizing into fluorescent DCF, the intensity of which was linearly related to the number of ROS produced. (B–C) Cells, some undergoing 1-h pretreatment with ROS inhibitor (NAC, 1 mM), were subject to 24-h GT treatment (300 μg/mL). (B) Cell viability was evaluated through the MTT assay. (C) Western blotting was used to identify the extent of LC3-I to LC3-II conversion. Relative protein band intensity changes were calculated using commercially available software (control; 1-fold increase). Data are reported as the mean ± SD of three experiments. $^*p < 0.05$; $^{**}p < 0.01$; $^{***}p < 0.001$ relative to untreated cells.

3.10. GT dysregulates the Bax/Bcl-2 and Beclin-1/Bcl-2 ratio

Apoptosis and prolonged autophagy are two processes involved in cell death. Proteins Bcl-2 and Beclin-1 indicate the occurrence of apoptosis and autophagy, respectively (Marquez and Xu, 2012). The influence of GT on Bcl-2 (antiapoptotic) protein was investigated, and the role of Bcl-2 protein in Bax (proapoptotic) and Beclin-1 (proautophagic) protein expression within K562 cells was determined. Western blotting revealed time-dependent downregulation of Bcl-2 expression when GT treatment was applied (300 μg/mL, for 2–24 h; Fig. 9A). No simultaneous changes in the expression of Bax protein were observed (Fig. 9A). Furthermore, when GT was applied, Beclin-1 protein expression was found to dramatically increase with time (Fig. 9A). The lack of Bcl-2 when GT was present may have promoted

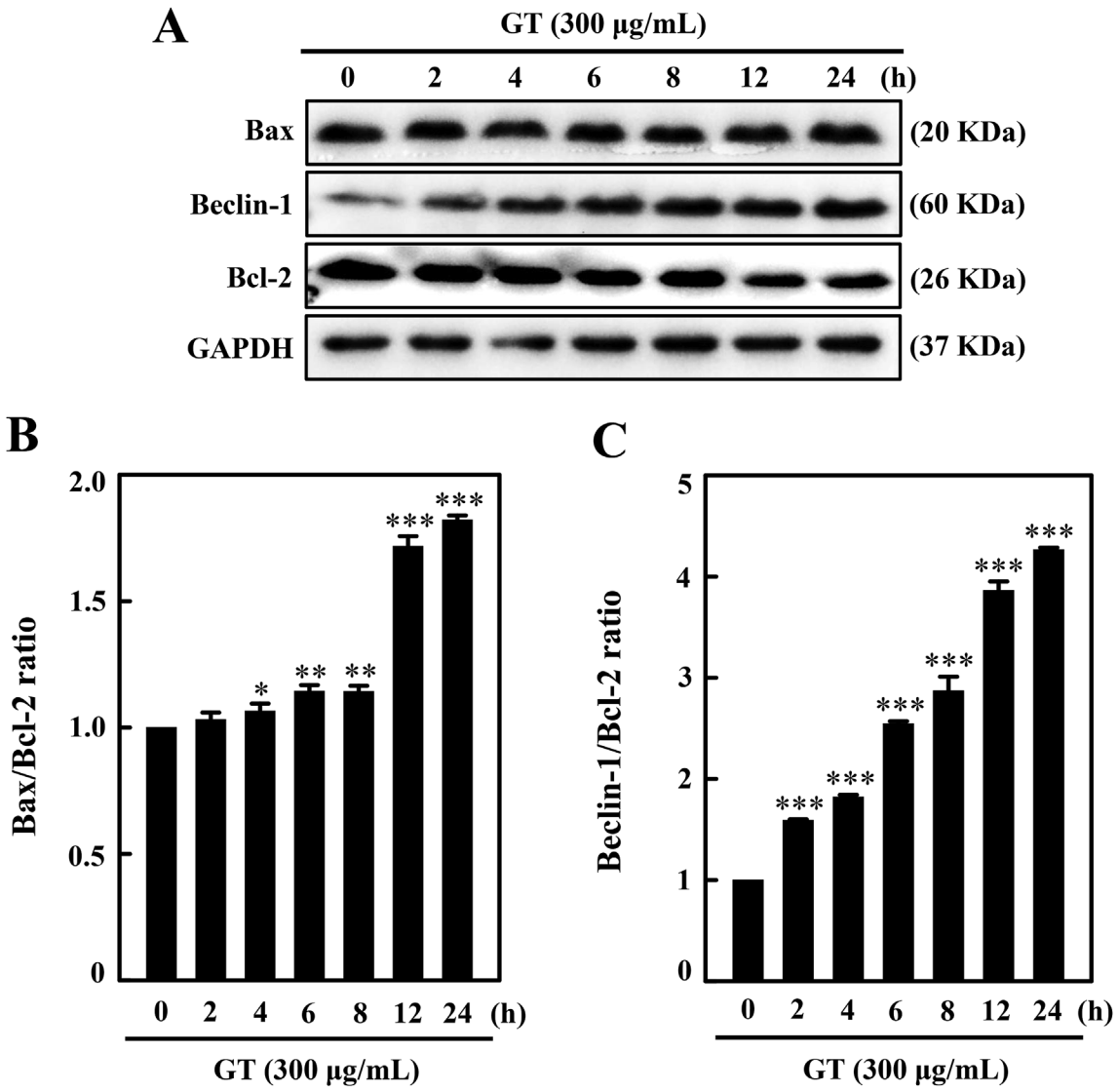

Fig. 9. The Bax/Bcl-2 and Beclin-1/Bcl-2 ratios in K562 cells were increased by GT treatment. (A) Western blotting was used to determine the time-dependent effects of GT on Bax, Beclin-1 and Bcl-2 protein levels. (B–C) Relative changes in the Bax/Bcl-2 and Beclin-1/Bcl-2 ratios were evaluated using commercial quantitative software (control; 1-fold increase). Data are reported as the mean ± SD of three experiments. *$p < 0.05$; **$p < 0.01$; ***$p < 0.001$ relative to untreated cells.

autophagy and apoptosis in K562 cells. The Bax/Bcl-2 and Beclin-1/Bcl-2 ratios exponentially increased over time with GT treatment (Fig. 9B and C), which suggested the favoring of both apoptosis and autophagy.

3.11. Inhibition of cytoprotective autophagy enhances GT-induced apoptosis in K562 cells

To examine the interference of GT in the interaction between apoptosis and autophagy, we evaluated apoptosis by treating the cells with 1 mM 3-MA or 20 μM CQ, which are inhibitors of early and late autophagy, respectively. Pretreatment with 3-MA suppressed LC3-II accumulation (Fig. 10A and B), whereas that with CQ promoted LC3-II accumulation (Fig. 10C and D). both autophagy inhibitors enhanced caspase-3 activation in K562 cells (Fig. 10A–D). These findings fully explain the inhibitors' effect on GT-induced cytoprotective autophagy, which is to enhance GT-induced caspase-3 activation, leading to enhanced cell death.

3.12. Inhibition of apoptosis did not affect GT-induced autophagy in K562 cells

Caspases are usually in inactive form, and activating caspases is crucial to apoptosis execution. To demonstrate the interference of GT in the apoptosis–autophagy interaction, we treated cells with an inhibitor of apoptosis (Z-VAD-FMK) and identified the consequent changes in LC3-I/LC3-II colocalization and caspase-3 activation by using Western blotting. Intriguingly, the inhibiting effect of Z-VAD-FMK on caspase-3 activation did not affect the degree of LC3-II accumulation against GT-induced apoptosis in K562 cells (Fig. 10E and F). This finding revealed that Z-VAD-FMK inhibited apoptosis but did not affect GT-induced autophagy.

3.13. EGFR and PI3K/AKT/mTOR inhibition and cytoprotective autophagy activation in GT-treated K562 cells

PI3K/AKT/mTOR signaling cascades have been demonstrated to be strongly promoted by overexpression of EGFR, and such promotion is responsible for regulating different types of tumors (Komoto et al., 2009). A dynamic and self-catabolic process in cells, autophagy is

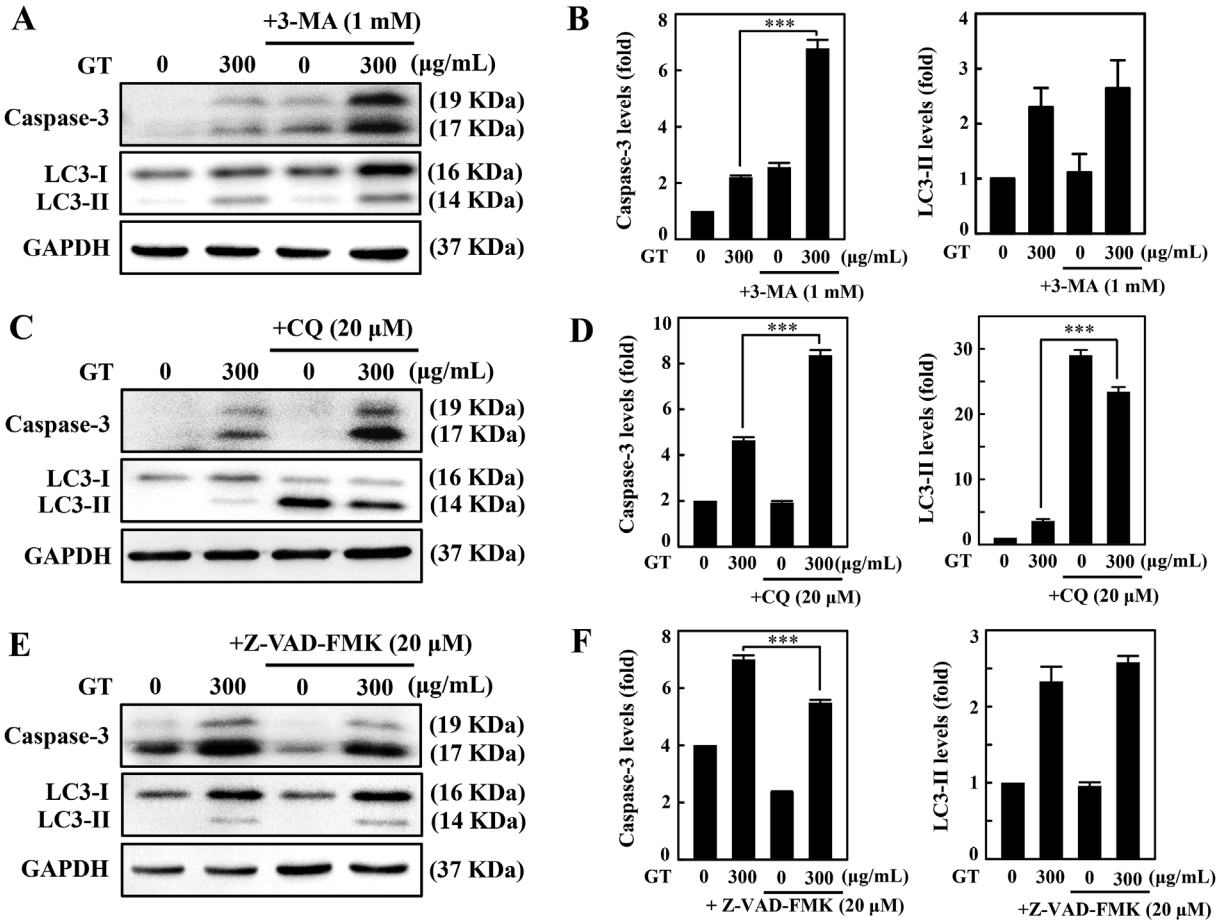

Fig. 10. Interplay in K562 cells between GT-induced autophagy and apoptosis. (A) Cells, some undergoing 1-h pretreatment with 3-MA, were subject to 24-h incubation with GT (300 μg/mL). Western blotting was employed to determine the degree of conversion of LC3-I to LC3-II and caspase-3 cleavage. (B) Protein band intensity changes were determined on commercial quantitative software (control; 1-fold increase). (C) Cells, some undergoing 1-h pretreatment with CQ, were subject to 24-h incubation with GT (300 μg/mL). Western blotting was employed to determine the degree of conversion of LC3-I to LC3-II and caspase-3 cleavage. (D) Relative protein band intensity changes were determined on commercial available quantitative software (control; 1-fold). (E) Cells, some undergoing 1-h pretreatment with Z-VAD-FMK, were subjected to 24-h incubation with GT (300 μg/mL). Western blotting was employed to determine the degree of conversion of LC3-I to LC3-II and caspase-3 cleavage. (F) Relative protein band intensity changes were determined on commercial available quantitative software (control; 1-fold increase). Data are reported as the mean ± SD of three experiments. $*p < 0.05$; $**p < 0.01$; $***p < 0.001$ relative to untreated cells.

subject to strict regulation by upstream modulators; that is, by the PI3K/AKT/mTOR signaling pathway (Jain et al., 2013). GT treatment significantly inhibited phosphorylated EGFR levels in K562 cells (Fig. 11A). We sought to discover the effects of GT treatment on the downstream proteins PI3K, AKT, and mTOR. GT treatment was demonstrated using Western blotting to significantly and dose-dependently attenuate the phosphorylation of these three proteins in K562 cells (Fig. 11B). Interestingly, we discovered that LY294002

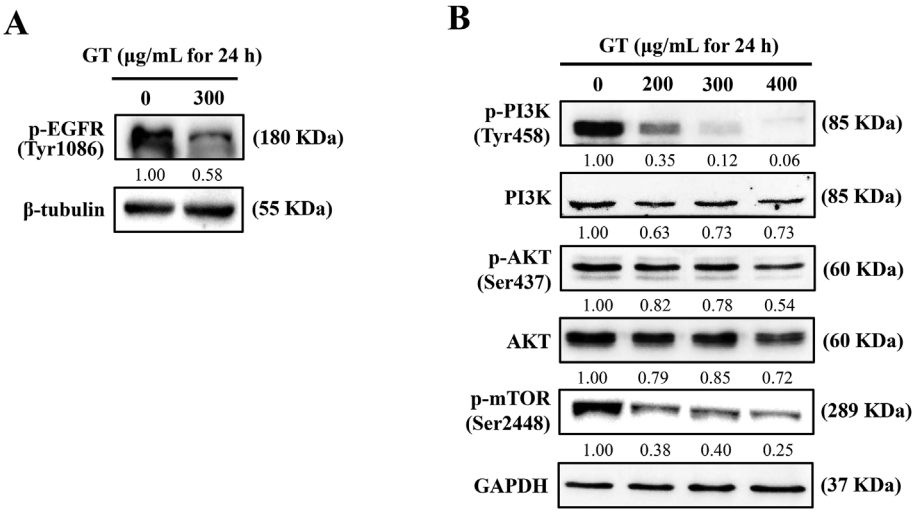

Fig. 11. Inhibitory effects of GT on phosphorylation of EGFR, PI3K, AKT and mTOR signaling pathways in K562 cells. (A) Cells underwent 24-h GT treatment (300 μg/mL). Immunoblotting was employed to measure p-EGFR levels. (B) Cells underwent 24-h incubation with GT (200–400 μg/mL). Immunoblotting was performed to measure p-PI3K, PI3K, p-AKT, AKT, and p-mTOR levels. (C) Cells, some undergoing 1-h pretreatment with LY294002 (20 μM), were subject to 24-h GT treatment (200–400 μg/mL). Cell viability was assayed using MTT assay. Data are reported as the mean ± SD of three experiments. $*p < 0.05$; $**p < 0.01$; $***p < 0.001$ relative to untreated cells.

pretreatment reversed GT-induced cell death in K562 cells (Fig. 11C). GT was thus found to suppress EGFR expression and the PI3K/AKT/mTOR signaling cascade, activating cytoprotective autophagy in K562 cells.

4. Discussion

The search for anticancer therapy employing phytocompounds has attracted considerable interest in the field of cancer biology. Medicinal mushroom extracts have been shown both *in vitro* and *in vivo* to have potential antitumor properties in various types of cancer cells. GT can arrest apoptosis and S-phase cell-cycle progression in adenocarcinoma cells of the lung (Yu et al., 2012). Few researchers have studied the anticancer effects of GT against human CML. In this study, we showed that ethanol extracts of GT could suppress the growth of K562 cells through G_2/M phase cell-cycle arrest; additionally, we discovered GT to induce apoptosis and autophagy in K562 cells by downregulating EGFR/PI3K/AKT/MTOR signaling molecules.

The cell cycle is a principal regulator of growth and division of cells. A helpful strategy for halting tumor growth is to perturb cell-cycle progression (Williams and Stoeber, 2011). Arrest of the cycle during the G_2/M phase can be triggered by various cellular stresses. Cell-cycle arrest in tumor cells leads to either repair or apoptosis. Strong inhibitory effects on cancer cells, achieved through disrupting cell-cycle progression or inducing cell apoptosis, are exhibited only by a few medicinal mushrooms (Patel and Goyal, 2012). Studies have demonstrated that GT hinders the proliferation of cells by arresting the G_2/M phase cell cycle in Hep3B hepatoma and COLO205 colorectal cancer cells (Gan et al., 1998; Hsu et al., 2008), the S phase in H23/0.3 lung adenocarcinoma cells (Yu et al., 2012), and the G_1 phase in BT-474 breast cancer cells and HER-2-overexpressing SKOV-3 ovarian cancer (Kuo et al., 2013). Consistent with previous studies, we observed that GT treatment caused K562 cells to accumulate in the G_2/M phase (Fig. 2B).

Apoptosis is the primary form of cell death and serves as a potential target for preventing the proliferation of malignant tumor cells (Guicciardi and Gores, 2009). Medicinal-mushroom-triggered apoptosis has gained considerable attention in comparison with well-established mammalian apoptosis; however, the signaling pathways linked to apoptosis in GT-treated cells remain to be elucidated. Our results suggest that K562 cells treated with varying concentrations of GT had a significantly higher rate of apoptosis than similarly treated U937 and HL-60 cells (Figs. 1 and 3). Experimental evidence is mounting that either mitochondrial (intrinsic) or death receptor (extrinsic) pathways trigger apoptosis. The mitochondrial/caspase-mediated signaling cascade is a principal pathway of apoptosis, and mitochondrial outer-membrane permeabilization (MOMP) has a strong role in this pathway. The collapse of MOMP leads to cytochrome c release into cytoplasm, which triggers the caspase cascade and subsequent apoptosis (Earnshaw et al., 1999; Xiong et al., 2014). We found that GT treatment upregulated cytochrome c and procaspase-9/-3 and proteolytically cleaved PARP, which led to apoptotic cell death in K562 cells (Fig. 4A). Regulation of the death-receptor-mediated extrinsic pathway is activated through the expression of FasL, Fas and caspase-8, and such expression sequentially promotes apoptosis. Caspase-8 activation triggers the proteolytic cleavage of mitochondrial-associated Bid to induce apoptotic cell death following death receptor (FasL) activation (Kaufmann et al., 2012). Mitochondrial membrane permeabilization is targeted by Bid, a proapoptotic protein that is a substrate for caspase-8 (Kantari and Walczak, 2011). Bid thus connects the extrinsic and intrinsic pathways of apoptosis (Schug et al., 2011). GT-treatment-induced apoptosis was discovered in the present study to be involved in the activation of Fas, cleavage of caspase-8 into an active form, and cleavage of Bid in K562 cells, with the effects of GT treatment found to be concentration dependent (Fig. 4B). Overall, the findings presented herein suggest that GT-induced apoptosis is mediated through extrinsic and intrinsic pathways. Although the mitochondria potential was lower when GT treatment was applied (Fig. 4C and D), when cells were treated with the antioxidant NAC, an apoptosis blocker, no significant differences were noted compared with the GT-treated sample, suggesting an independent ROS pathway.

The relationship between ROS and apoptosis has been well documented (Circu and Aw, 2010). Apoptosis can be induced by ROS accumulation in live cells, and this accumulation has been implicated in the activation of various transcriptional factors eventually resulting in apoptosis (Wiseman and Halliwell, 1996; Simon et al., 2000). Pretreating K562 cells with NAC (1 mM), an ROS inhibitor, and GT extract (400 μg/mL) resulted in non-significant different rates of early/late apoptosis (Fig. 5A and B). This finding suggests that early/late apoptosis is ROS independent, corroborating our other findings (Fig. 4C and D).

Autophagy, or self-eating, is a process associated with the destruction and recycling of macromolecules and organelles, which serve various functions in myeloid leukemia and solid tumors (Zhang et al., 2013). During autophagy, LC3-II is formed by the conjoining of a cytosolic form of LC3 (LC3-I) to phosphatidylethanolamine, which is achieved through Atg7 and Atg3, which are activating enzymes (Jiang and Mizushima, 2015). Sequestosome 1 (SQSTM1), which is another crucial protein and is also known as p62, directly binds to LC3-II through a specific sequence motif and in the process forming autophagosomes then undergoes self-degradation during autophagy (Moscat and Diaz-Meco, 2009). p62/SQSTM1 is an autophagy adaptor protein that functions as a signaling hub; this is possible because it can interact with signaling proteins (Moscat and Diaz-Meco, 2009). The upregulation of p62/SQSTM1 constitutes a survival mechanism in mature acute myeloid leukemia cells (Trocoli et al., 2014). Puissant et al. (2010) reported that p62 accumulation is required in myelogenous leukemia cells if resveratrol is to induce autophagy. Consistent with those detailed in previous reports, the data obtained from the current study demonstrated that GT treatment of K562 cells triggered autophagy by increasing the amount of LC3-II accumulated, the amount of AVOs formed, and P62/SQSTM1 expression (Fig. 6A, C, and D). Concomitantly, the RT-PCR results showed upregulation of LC3 mRNA expression levels (Fig. 6B). These findings suggest that GT treatment promotes autophagy in K562 leukemia cells.

Autophagy and apoptosis-associated cell-death mechanisms play a pivotal role in tumor suppression. Programmed cell death is classified as Type I or II, apoptosis and autophagy, respectively and these two types are present in the same cell and share some common key signaling cascades in promoting cell survival or death. The two cellular processes can mutually regulate the other in an inhibitory manner (Mariño et al., 2014). Autophagy inhibitors such as 3-MA and CQ have been used to delineate the antitumor properties of compounds derived from nature and traditional Chinese medicine extracts (Wang et al., 2014; Iqbal et al., 2017). Our results revealed autophagy inhibition through the pharmacological inhibitor 3-MA or CQ to enhance caspase-3 cleavage, indicating that GT-mediated cytoprotective autophagy impeded GT-induced apoptosis in K562 cells (Fig. 7A and B).

Overproduction of ROS in cancer cells lead to the initiation and promotion of cell death through apoptosis or autophagy (Bazhin et al., 2016). Studies have reported that medicinal mushroom extracts trigger the formation of ROS in breast cancer cells (Wang et al., 2017) and human promyelocytic leukemia cells (Hseu et al., 2014). By contrast, our study demonstrated that GT incubation did not generate ROS in K562 cells (Fig. 8A and B). In addition, pretreatment with the ROS inhibitor NAC did not affect the degree of apoptosis and LC3-II accumulation that was induced by GT treatment (Fig. 8C). These findings confirm that ROS were not involved in GT-induced apoptosis or cytoprotective autophagy in K562 cells.

A major apoptotic pathway of the signal transduction cascade that is involved in programmed cell death contains members of the family of Bcl-2 proteins, and these proteins regulate apoptosis through their

mutual interaction (Tsujimoto, 2003). The role of the Bax/Bcl-2 ratio in apoptotic cell-death mechanisms has been evaluated in several studies and found to be crucial to whether apoptosis is triggered. Proportional to the resistance (or relative sensitivity) to diverse apoptotic stimuli (Huang et al., 2008), the Bax/Bcl-2 ratio appears to be a critical cellular threshold factor determining whether apoptosis proceeds through the mitochondrial pathway. Our results showed that GT treatment exponentially increased the Bax/Bcl-2 ratio, which triggered progression of apoptotic cell death in K562 cells (Fig. 9B). Beclin-1 is considered a crucial protein in the pathway governing autophagy, and its expression level might be cytoprotective or promoting apoptosis cell death. Bcl-2, a critical autophagy inhibitor, is known to inhibit Beclin-1 under normal conditions. In response to stress, Beclin-1 dissociates from Bcl-2, leading to the triggering of autophagy (Pattingre et al., 2005). We observed that incubation with GT markedly increased Beclin-1/Bcl-2 expression levels in a time-dependent experiment (2, 4, 6, 8, 12, and 24 h), demonstrating the triggering of autophagy in K562 cells (Fig. 9A–C). Collectively, our findings demonstrated that in K562 cells, GT induced autophagy and apoptosis.

EGFR and PI3K/AKT/mTOR, pathway, is considered as an attractive target for the development of anti-cancer drugs. Overexpression of EGFR activates the aforementioned signaling pathway, resulting in uncontrolled cell growth and survival. In such circumstances, cancer cells have a competitive growth advantage and exhibit therapy resistance, angiogenesis, and metastatic competence (Porta et al., 2014). Inhibition of the PI3K/AKT/mTOR signaling pathway has been revealed to promote autophagy in cancer cells (Shao et al., 2016; Chang et al., 2017). A dynamic and self-catabolic process, autophagy is subject to strict regulation by upstream modulators; that is, principally by the PI3K/AKT/mTOR signaling pathway. In cancer cells, natural bioactive compounds induce autophagy through this pathway (Sun et al., 2013). Therefore, inhibition of EFGR and the PI3K/AKT/mTOR signaling cascade could promote autophagy in cancer cells. GT incubation was discovered in this study to effectively decrease the protein expression of EFGR, phosphorylated EGFR, PI3K, phosphorylated PI3K, AKT, and phosphorylated AKT (Fig. 11 A and B). However, LY294002 pretreatment reversed GT-induced cell death in K562 cells (Fig. 11C). These findings may suggest that GT inhibits EGFR and PI3K/AKT/mTOR to activate cytoprotective autophagy in K562 cells. Similarly, a recent study found that deoxypodophyllotoxin downregulated the PI3K/AKT/mTOR pathway to induce cytoprotective autophagy against apoptosis in osteosarcoma U2OS cells (Kim et al., 2017). In summary, findings show that GT can activate cytoprotective autophagy against apoptosis in human leukemia K562 cancer cells.

Ganoderma tsugae is known to have multifaceted properties like anticancer (Kuo et al., 2013; Hsu et al., 2008; Yu et al., 2012), anti-inflammatory (Ko et al., 2008) and anti-fibrotic properties (Zhou et al., 2007) with low toxicity or no side effects. For instance grape seed extract a well known anti-cancer agent (Sahpazidou et al., 2014) could induce side effects like nausea, headache, and risky for people with high blood pressure as well as they interfere with certain drugs taken by patients (National Institutes of Health, September 2016). For these reason GT was determined to be a suitable candidate as an anti-cancer agent.

5. Conclusion

This study is the first to demonstrate that both apoptosis and autophagy can be induced in human CML K562 cells using GT and that GT-induced autophagy mediates the cytoprotective role. Cancer researchers are continually searching for new therapeutic targets, of which cell-cycle arrest and apoptosis have become among them. Our findings, therefore, offer novel insight into the molecular mechanisms behind cytoprotective autophagy and apoptosis in K562 cells. Our research suggests GT combined with autophagy inhibition as a potential new therapeutic strategy for improving treatment of human CML.

Conflicts of interest

The authors have no conflicts of interest to declare.

Acknowledgments

The grants MOST-106-2320-B-039-054-MY3 and MOST-104-2320-B-039-040-MY3 from the Ministry of Science and Technology, Taiwan as well as by the "Chinese Medicine Research Center, China Medical University" from the Featured Areas Research Center Program within the framework of the Higher Education Sprout Project by the Ministry of Education in Taiwan (CMRC-CHM-9) supported this work.

Transparency document

Transparency document related to this article can be found online at https://doi.org/10.1016/j.fct.2018.11.043.

References

Bazhin, A.V., Philippov, P.P., Karakhanova, S., 2016. Reactive oxygen species in cancer biology and anticancer therapy. Oxidative Medicine and Cellular Longevity 4197815 2016.
Circu, M.L., Aw, T.Y., 2010. Reactive oxygen species, cellular redox systems and apoptosis. Free Radical Biol. Med. 48 (6), 749–762.
Chang, C.T., Hseu, Y.C., Thiyagarajan, V., Huang, H.C., Hsu, L.S., Huang, P.J., Liu, J.Y., Liao, J.W., Yang, H.L., 2017. *Antrodia salmonea* induces G 2 cell-cycle arrest in human triple-negative breast cancer (MDA-MB-231) cells and suppresses tumor growth in athymic nude mice. J. Ethnopharmacol. 196, 9–19.
Chen, M.L., Lin, B.F., 2007. Effects of triterpenoid-rich extracts of *Ganoderma tsugae* on airway hyperreactivity and Th2 responses in vivo. Int. Arch. Allergy Immunol. 143, 21–30.
Earnshaw, W.C., Martins, L.M., Kaufmann, S.H., 1999. Mammalian caspases: structure, activation, substrates, and functions during apoptosis. Annu. Rev. Biochem. 68, 383–424.
Gan, K.H., Fann, Y.F., Hsu, S.H., Kuo, K.W., Lin, C.N., 1998. Mediation of the cytotoxicity of lanostanoids and steroids of *Ganoderma tsugae* through apoptosis and cell cycle. J. Nat. Prod. 61, 485–487.
Gozuacik, D., Kimchi, A., 2004. Autophagy as a cell death and tumor suppressor mechanism. Oncogene 23, 2891–2906.
Grape Seed Extract, September 2016. Herbs at a Glance. US National Center for Complementary and Integrative Health, National Institutes of Health.
Guicciardi, M.E., Gores, G.J., 2009. Life and death by death receptors. Fed. Am. Soc. Exp. Biol. 23 (6), 1625–1637.
Hseu, Y.C., Chen, S.C., Chen, H.C., Liao, J.W., Yang, H.L., 2008. *Antrodia camphorata* inhibits proliferation of human breast cancer cells in vitro and in vivo. Food Chem. Toxicol. 46, 2680–2688.
Hseu, Y.C., Lee, C.C., Chen, Y.C., Kumar, K.J., Chen, C.S., Huang, Y.C., Hsu, L.S., Huang, H.C., Yang, H.L., 2014. The anti-tumor activity of *Antrodia salmonea* in human promyelocytic leukemia (HL-60) cells is mediated via the induction of G_1 cell-cycle arrest and apoptosis in vitro or in vivo. Journal of Ethanopharmacology 153 (2), 499–510.
Hsu, S.C., Ou, C.C., Chuang, T.C., Li, J.W., Lee, Y.J., Wang, V., Liu, J.Y., Chen, C.S., Lin, S.C., Kao, M.C., 2009. *Ganoderma tsugae* extract inhibits expression of epidermal growth factor receptor and angiogenesis in human epidermoid carcinoma cells: in vitro and in vivo. Cancer Lett. 281, 108–116.
Hsu, S.C., Ou, C.C., Li, J.W., Chuang, T.C., Kuo, H.P., Liu, J.Y., Chen, C.S., Lin, S.C., Su, C.H., Kao, M.C., 2008. *Ganoderma tsugae* extracts inhibit colorectal cancer cell growth via G 2/M cell cycle arrest. J. Ethnopharmacol. 120, 394–401.
Huang, X.F., Luo, S.K., Xu, J., Li, J., Xu, D.R., Wang, L.H., Yan, M., Wang, X.R., Wan, X.B., Zheng, F.M., Zeng, Y.X., Liu, Q., 2008. Aurora kinase inhibitory VX-680 increases Bax/Bcl-2 ratio and induces apoptosis in Aurora-A-high acute myeloid leukemia. Blood 111 (5), 2854–2865.
Iqbal, J., Abbasi, B.A., Mahmood, T., Kanwal, S., Ali, B., Shah, S.A., Khali, A.T., 2017. Plant-derived anticancer agents: a green anticancer approach. Asian Pacific Journal of Tropical Biomedicine 7 (12), 1129–1150.
Jain, K., Paranandi, K.S., Sridharan, S., Basu, A., 2013. Autophagy in breast cancer and its implications for therapy. American journal of cancer research 3, 251.
Jiang, P., Mizushima, N., 2015. LC3- and p62-based biochemical methods for the analysis of autophagy progression in mammalian cells. Methods 75, 13–18.
Kabeya, Y., Mizushima, N., Ueno, T., Yamamoto, A., Kirisako, T., Noda, T., Kominami, E., Ohsumi, Y., Yoshimori, T., 2000. LC3, a mammalian homologue of yeast Apg8p, is localized in autophagosome membranes after processing. EMBO J. 19, 5720–5728.
Kantari, C., Walczak, H., 2011. Caspase-8 and bid: caught in the act between death receptors and mitochondria. Biochim. Biophys. Acta 1813 (4), 558–563.
Kaufmann, T., Strasser, A., Jost, P.J., 2012. Fas death receptor signalling: roles of Bid and XIAP. Cell Death. Differ. 19, 42–50.
Khajapeer, K.V., Baskaran, R., 2016. Natural Products for Treatment of Chronic Myeloid Leukemia, Anti-cancer Drugs-nature, Synthesis and Cell. InTech open, United Kingdom. https://doi.org/10.5772/6617.
Kim, S.H., Son, K.M., Kim, K.Y., Yu, S.N., Park, S.G., Kim, Y.W., Nam, H.W., Suh, J.T., Ji,

J.H., Ahn, S.C., 2017. Deoxypodophyllotoxin induces cytoprotective autophagy against apoptosis via inhibition of PI3K/AKT/mTOR pathway in osteosarcoma U2OS cells. Pharmacol. Rep. 69, 878–884.
Ko, H.H., Hung, C.F., Wang, J.P., Lin, C.N., 2008. Antiinflammatory triterpenoids and steroids from *Ganoderma lucidum* and *G. tsugae*. Phytochemistry 69, 234–239.
Komoto, M., Nakata, B., Amano, R., Yamada, N., Yashiro, M., Ohira, M., Wakasa, K., Hirakawa, K., 2009. HER2 overexpression correlates with survival after curative resection of pancreatic cancer. Cancer Sci. 100, 1243–1247.
Kondo, Y., Kanzawa, T., Sawaya, R., Kondo, S., 2005. The role of autophagy in cancer development and response to therapy. Nat. Rev. Canc. 5, 726–734.
Kuo, H.P., Hsu, S.C., Ou, C.C., Li, J.W., Tseng, H.H., Chuang, T.C., Liu, J.Y., Chen, S.J., Su, M.H., Cheng, Y.C., 2013. *Ganoderma tsugae* extract inhibits growth of HER2-overexpressing cancer cells via modulation of HER2/PI3K/Akt signaling pathway. Evid. base Compl. Alternative Med. 2013, 219472.
Kuok, Q.Y., Yeh, C.Y., Su, B.C., Hsu, P.L., Ni, H., Liu, M.Y., Mo, F.E., 2013. The triterpenoids of *Ganoderma tsugae* prevent stress-induced myocardial injury in mice. Food & Function 57 (10), 1892–1896.
Lin, J.Y., Chen, M.L., Chiang, B.L., Lin, B.F., 2006. *Ganoderma Tsugae* supplementation alleviates bronchoalveolar inflammation in an airway sensitization and challenge mouse model. Int. Immunopharm. 6 (2), 241–251.
Lu, C.C., Hsu, Y.J., Chang, C.J., Lin, C.S., Martel, J., Ojcius, D.M., Ko, Y.F., Lai, H.C., Young, J.D., 2016. Immunomodulatory properties of medicinal mushrooms: differential effects of water and ethanol extracts on NK cell-mediated cytotoxicity. Innate Immun. 22 (7), 522–533.
Ly, J.D., Grubb, D.R., Lawen, A., 2003. The mitochondrial membrane potential (Δψm) in apoptosis; an update. Apoptosis 8, 115–128.
Maiuri, M.C., Zalckvar, E., Kimchi, A., Kroemer, G., 2007. Self-eating and self-killing: crosstalk between autophagy and apoptosis. Nat. Rev. Mol. Cell Biol. 8, 741–752.
Mariño, G., Niso-Santano, M., Baehrecke, E.H., Kroemer, G., 2014. Self-consumption: the interplay of autophagy and apoptosis. Nat. Rev. Mol. Cell Biol. 15 (2), 81–94.
Marquez, R.T., Xu, L., 2012. Bcl-2:Beclin 1 complex: multiple, mechanisms regulating autophagy/apoptosis toggle switch. American Journal of Cancer Research 2 (2), 214–221.
Morselli, E., Galluzzi, L., Kepp, O., Vicencio, J.M., Criollo, A., Maiuri, M.C., Kroemer, G., 2009. Anti-and pro-tumor functions of autophagy. Biochim. Biophys. Acta Mol. Cell Res. 1793, 1524–1532.
Moscat, J., Diaz-Meco, M.T., 2009. p62 at the crossroads of autophagy, apoptosis, and cancer. Cell 137, 1001–1004.
Nowell, P.C., 2007. Discovery of the Philadelphia chromosome: a personal perspective. JCI (J. Clin. Investig.) 117 (8), 2033–2035.
Pan, M.H., Chen, W.J., Lin-Shiau, S.Y., Ho, C.T., Lin, J.K., 2002. Tangeretin induces cell-cycle G1 arrest through inhibiting cyclin-dependent kinases 2 and 4 activities as well as elevating Cdk inhibitors p21 and p27 in human colorectal carcinoma cells. Carcinogenesis 23, 1677–1684.
Pattingre, S., Tassa, A., Qu, X., Garuti, R., Liang, X.H., Mizushima, N., Packer, M., Schneider, M.D., Levine, B., 2005. Bcl-2 antiapoptotic proteins inhibit Beclin 1-dependent autophagy. Cell 122 (6), 927–939.
Park, S.H., Kim, J.H., Chi, G.Y., Kim, G.Y., Chang, Y.C., Moon, S.K., Nam, S.W., Kim, W.J., Yoo, Y.H., Choi, Y.H., 2012. Induction of apoptosis and autophagy by sodium selenite in A549 human lung carcinoma cells through generation of reactive oxygen species. Toxicol. Lett. (Shannon) 212, 252–261.
Patel, S., Goyal, A., 2012. Recent developments in mushrooms as anti-cancer therapeutics: a review. Biotec 3 (2), 1–15.
Porta, C., Paglino, C., Mosca, A., 2014. Targeting PI3K/Akt/mTOR signaling in cancer. Frontiers in Oncology 4, 64.
Puissant, A., Fenouille, N., Auberger, P., 2012. When autophagy meets cancer through p62/SQSTM1. Am. J. Cancer Res. 2 (4), 397–413.
Ricci, M.S., Zong, W.X., 2006. Chemotherapeutic approaches for targeting cell death pathways. Oncol. 11, 342–357.
Sahpazidou, D., Geromichalos, G.D., Stagos, D., Apostolou, A., Haroutouian, S.A., Tsarsakis, A.M., Tzanakakis, N.G., Hayes, A.W., Kouretas, D., 2014. Anticarcinogenic activity of polyphenolic extracts from grape stems against breast, colon, renal and thyroid cancer cells. Toxicol. Lett. 230, 218–224.
Schug, Z.T., Gonzalvez, F., Houtkooper, R., Vaz, F.M., Gottlieb, E., 2011. BID is cleaved by caspase-8 within a native complex on the mitochondrial membrane. Cell Death Differ. 18, 538–548.
Shao, X., Lai, D., Zhang, L., Xu, H., 2016. Induction of autophagy and apoptosis via PI3K/AKT/TOR pathways by azadirachtin a in spodoptera litura cells. Sci. Rep. 6, 35482.
Sharma, R., 2012. Cancer chemoprevention: prevention is better than cure. J. Canc. Sci. Ther. 3, 1.
Simon, H.U., Haj-Yehia, A., Levi-Schaffer, F., 2000. Role of reactive oxygen species (ROS) in apoptosis induction. Apoptosis 5 (5), 415–418.
Su, C.H., Yang, Y.Z., Ho, H.O., Hu, C.H., Sheu, M.T., 2001. High-performance liquid chromatographic analysis for the characterization of triterpenoids from Ganoderma. J. Chromatogr. Sci. 39 (3), 93–100.
Sun, H., Wang, Z., Sebastian Yakisich, J., 2013. Natural products targeting autophagy via the PI3K/Akt/mTOR pathway as anticancer agents. Anti Cancer Agents Med. Chem. 13, 1048–1056.
Taylor, R.C., Cullen, S.P., Martin, S.J., 2008. Apoptosis: controlled demolition at the cellular level. Nat. Rev. Mol. Cell Biol. 9, 231–241.
Trocoli, A., Bensadoun, P., Richard, E., Labrunie, G., Merhi, F., Schläfli, A.M., Brigger, D., Souquere, S., Pierron, G., Pasquet, J.M., Soubeyran, P., Reiffers, J., Ségal-Bendirdjian, E., Tschan, M.P., Djavaheri-Mergny, M., 2014. p62/SQSTM1 upregulation constitutes a survival mechanism that occurs during granulocytic differentiation of acute myeloid leukemia cells. Cell Death & Differ. 21 (12), 1852–1861.
Tseng, Y.H., Yang, J.H., Mau, J.L., 2008. Antioxidant properties of polysaccharides from *Ganoderma tsugae*. Food Chem. 107, 732–738.
Tseng, H.H., Yeh, W.C., Tu, Y.C., Yang, B.F., Lai, Y.T., Lee, H.K., Yang, Y.C., Huang, H.C., Lee, Y.J., Ou, C.C., Kuo, H.P., Kuo, Y.H., Kao, M.C., Liu, J.Y., 2018. Proteomic profiling of *Ganoderma tsugae* ethanol extract-induced adipogenesis displaying browning features. FEBS Lett. 592 (10), 1643–1666.
Tsujimoto, Y., 2003. Cell death regulation by the Bcl-2 protein family in the mitochondria. J. Cell. Physiol. 195 (2), 158–167.
Wang, C.Y., Bai, X.Y., Wang, C.H., 2014. Traditional Chinese medicine: a treasured natural resource of anticancer drug research and development. Am. J. Chin. Med. 42, 543.
Wang, H.M., Yang, H.L., Thiyagarajan, V., Huang, T.-H., Huang, P.-J., Chen, S.-C., Liu, J.-Y., Hsu, L.S., Chang, H.W., Hseu, Y.C., 2017. Coenzyme Q0 enhances ultraviolet B–induced apoptosis in human estrogen receptor–positive breast (MCF-7) cancer cells. Integr. Canc. Ther. 16, 385–396.
Webb, K.C., Harasimowicz, M., Janeczek, M., Speiser, J., Swan, J., Tung, R., 2017. Development of asymmetric facial depigmentation in a patient treated with dasatinib with new-onset hypovitaminosis D: case report and review of the literature. Case Reports in Dermatological Medicine 5 2017.
Williams, G.H., Stoeber, K., 2011. The cell cycle and cancer. J. Pathol. 226 (2), 352–364.
Wiseman, H., Halliwell, B., 1996. Damage to DNA by reactive oxygen and nitrogen species: role in inflammatory disease and progression to cancer. Biochem. J. 313, 17–29.
Wu, G., Qian, Z., Guo, J., Hu, D., Bao, J., Xie, J., Xu, W., Lu, J., Chen, X., Wang, Y., 2012. *Ganoderma lucidum* extract induces G1 cell cycle arrest, and apoptosis in human breast cancer cells. Am. J. Chin. Med. 40, 631–642.
Xiong, S., Mu, T., Wang, G., Jiang, X., 2014. Mitochondria-mediated apoptosis in mammals. Protein & Cell. 5 (10), 737–749.
Yang, H.L., Lin, K.Y., Juan, Y.C., Kumar, K.S., Way, T.D., Shen, P.C., Chen, S.C., Hseu, Y.C., 2013. The anti-cancer activity of *Antrodia camphorata* against human ovarian carcinoma (SKOV-3) cells via modulation of HER-2/neu signaling pathway. J. Ethnopharmacol. 148, 254–265.
Yu, Y.H., Kuo, H.P., Hsieh, H.H., Li, J.W., Hsu, W.H., Chen, S.J., Su, M.H., Liu, S.H., Cheng, Y.C., Chen, C.Y., 2012. *Ganoderma tsugae* induces S phase arrest and apoptosis in doxorubicin-resistant lung adenocarcinoma H23/0.3 cells via modulation of the PI3K/Akt signaling pathway. Evid. base Compl. Alternative Med. 2012, 371286.
Yue, G.G., Fung, K.P., Tse, G.M., Leung, P.C., Lau, C.B., 2006. Comparative studies of various ganoderma species and their different parts with regard to their antitumor and immunomodulating activities in vitro. J. Alternative Compl. Med. 12, 777–789.
Zhang, J., 2013. Autophagy and mitophagy in cellular damage control. Redox Biol. 1, 19–23.
Zhou, X., Lin, J., Yin, Y., Zhao, J., Sun, X., Tang, K., 2007. Ganodermataceae: natural products and their related pharmacological functions. Am. J. Chin. Med. 35, 559–574.